Research Article

Yingying Jin, Liu Yang, Chenxinyu Pan, Zhangxing Shi, Bowen Cui, Peizhen Xu, Yuxin Yang, Ning Zhou, Xin Guo*, Pan Wang and Limin Tong*

Strong coupling of a plasmonic nanoparticle to a semiconductor nanowire

https://doi.org/10.1515/nanoph-2021-0214
Received May 4, 2021; accepted July 8, 2021;
published online July 22, 2021

Abstract: By placing a single Au nanoparticle on the surface of a cadmium sulfide (CdS) nanowire, we demonstrate strong coupling of localized surface plasmon resonance (LSPR) modes in the nanoparticle and whispering gallery modes (WGMs) in the nanowire. For a 50-nm-diameter Au-nanosphere particle, strong coupling occurs when the nanowire diameter is between 300 and 600 nm, with a mode splitting up to 80 meV. Using a temperature-induced spectral shift of the resonance wavelength, we also observe the anticrossing behavior in the strongly coupled system. In addition, since the Au nanosphere has spherical symmetry, the supported LSPR mode can be selectively coupled with transverse electric (TE) and transverse magnetic (TM) WGMs in the nanowire. The ultracompact strong-coupling system shown here may provide a versatile platform for studying hybrid "photon–plasmon" nanolasers, nonlinear optical devices, and nanosensors.

Keywords: Au nanoparticles; localized surface plasmon resonance; semiconductor nanowires; strong coupling; whispering gallery modes.

1 Introduction

Plasmonic nanoparticles, as typical plasmonic nanocavities [1–6], can support localized surface plasmon resonance (LSPR) and confine optical field into the nanoscale in all three dimensions [3], and have laid the foundation for applications including strong coupling [1, 2, 4–6], Raman spectroscopy [7, 8], and LSPR-based biosensors [9]. However, due to its intrinsic metal Ohmic loss and extremely small cavity size, an individually-used plasmonic nanoparticle typically suffers from short dephasing time of the coherent resonance [3], broad LSPR bandwidth, and difficulty in tailoring plasmonic characteristics, which may limit the performance of LSPR-based applications such as sensitivity in optical sensing [9], threshold in nanoplasmonic lasing [10–12] and nonlinear optical effects [13]. Strong coupling of a localized plasmonic mode to a low-loss photonic mode in a hybrid plasmonic–photonic cavity [14–17] provides a promising solution to elongate the LSPR lifetime via coherent energy exchange and recirculation between the two otherwise uncoupled modes, and thus offers an opportunity to manipulate characteristics of the original modes, such as dephasing time [18], energy distribution [19], and damping pathways [16]. Among various photonic cavities, whispering-gallery-mode (WGM) cavity, owing to its high-quality factor [20, 21], strong and easily accessible surface evanescent fields [22], has been proven a versatile platform for exploiting strongly coupling with excitons [23, 24], atoms [25, 26], and ions [27]. When coupled to plasmonic cavities, as the bandwidth of the LSPR is relatively broad at optical frequency (e.g., tens of nanometers [3]), a relatively large mode splitting is required for identification and manipulation of the strong coupling effects, and therefore a small WGM cavity size is preferred to match the lifetime of the LSPR (e.g., ~10 fs). Previously, WGMs in a silica

Yingying Jin and **Liu Yang** contributed equally to this work.

***Corresponding authors: Xin Guo**, Interdisciplinary Center for Quantum Information, State Key Laboratory of Modern Optical Instrumentation, College of Optical Science and Engineering, Zhejiang University, Hangzhou 310027, China, E-mail: guoxin@zju.edu.cn. https://orcid.org/0000-0002-6130-2278; and **Limin Tong**, Interdisciplinary Center for Quantum Information, State Key Laboratory of Modern Optical Instrumentation, College of Optical Science and Engineering, Zhejiang University, Hangzhou 310027, China; and Collaborative Innovation Center of Extreme Optics, Shanxi University, Taiyuan 030006, China, E-mail: phytong@zju.edu.cn
Yingying Jin, Liu Yang, Chenxinyu Pan, Zhangxing Shi, Bowen Cui, Peizhen Xu, Yuxin Yang, Ning Zhou and Pan Wang, State Key Laboratory of Modern Optical Instrumentation, College of Optical Science and Engineering, Zhejiang University, Hangzhou 310027, China, E-mail: jinyingying@zju.edu.cn (Y. Jin), yl_photonics@zju.edu.cn (L. Yang), panchenxy@zju.edu.cn (C. Pan), phostone@zju.edu.cn (Z. Shi), bwcui@zju.edu.cn (B. Cui), xpzhen@zju.edu.cn (P. Xu), 21730059@zju.edu.cn (Y. Yang), msezhoun@zju.edu.cn (N. Zhou), nanopan@zju.edu.cn (P. Wang)

microfiber have been employed to strongly couple with an Au nanorod [17], however, limited by the relatively low refractive index of the silica glass (~1.46), the cavity size (i.e., the microfiber diameter) is much larger compared with the resonance wavelength.

Semiconductor nanowires grown by a bottom-up chemical vapor deposition (CVD) method [28] have high refractive indices and submicrometer diameters, and can offer atomic-level sidewall smoothness [29] that is much lower in surface roughness compared with other cavity structures fabricated by top–down lithography [21]. Previously, WGMs have been observed in semiconductor nanowires with diameter down to 270 nm [30], which is close to or smaller than the resonance wavelength of light. Also, compared with the circular cross section of a glass microfiber with amorphous structure, a single-crystal semiconductor nanowire typically has a polygon cross section.

In this letter, by depositing single Au nanospheres on the surface of a suspended CdS nanowire with high refractive index (~2.7), we demonstrate the strong coupling of a plasmonic nanoparticle to a semiconductor nanowire at room temperature. Large mode splitting is observed with nanowire diameter down to 300 nm, much smaller than the resonance wavelength of ~530 nm. Using a temperature-induced spectral shift of the resonance wavelength, we observe anticrossing behavior in these strongly coupled systems. Besides, the dependence of coupling behavior on wire diameter has also been investigated.

2 Structure and fabrication

The hybrid strong coupling system is schematically illustrated in Figure 1a. An Au nanosphere deposited on one of the six sidewalls of a CdS wire is used as a nanoplasmonic resonator for concentrating light through LSPR and coupling it into WGMs of the hexagonal cavity. When the resonant frequencies of the two cavities are matched, and energy exchange between the two cavities is efficient enough, strong coupling between the LSPR modes and the WGMs may occur. Experimentally, CdS wires were synthesized via a CVD method [28]. By controlling the growth temperature and pressure, single-crystal CdS wires with diameters ranging from 100 nm to 2 μm and lengths up to 0.5 mm were obtained (see Figure S1a in the Supplementary Material). As-grown CdS wires exhibit high crystallization quality and hexagonal cross section (see inset of Figure 1b and Figure S1b–d in the Supplementary Material). Figure 1b shows a typical dark-field scattering spectrum of a 1.5-μm-diameter CdS wire. Illuminated by a broadband white light (EQ-99, ENERGETIQ, see the spectrum of the white light in Figure S2 in the Supplementary Material) filtered by a 500-nm long-pass filter (FEL0500, Thorlabs), the wire gives clear resonance modes, agreeing well with that of a hexagonal WGM microcavity [31]. Au nanospheres were chemically synthesized using a seed-mediated method and are relatively uniform in sizes with an average diameter of 50 ± 5 nm (see Figure S3 in the Supplementary Material). Figure 1c shows a typical

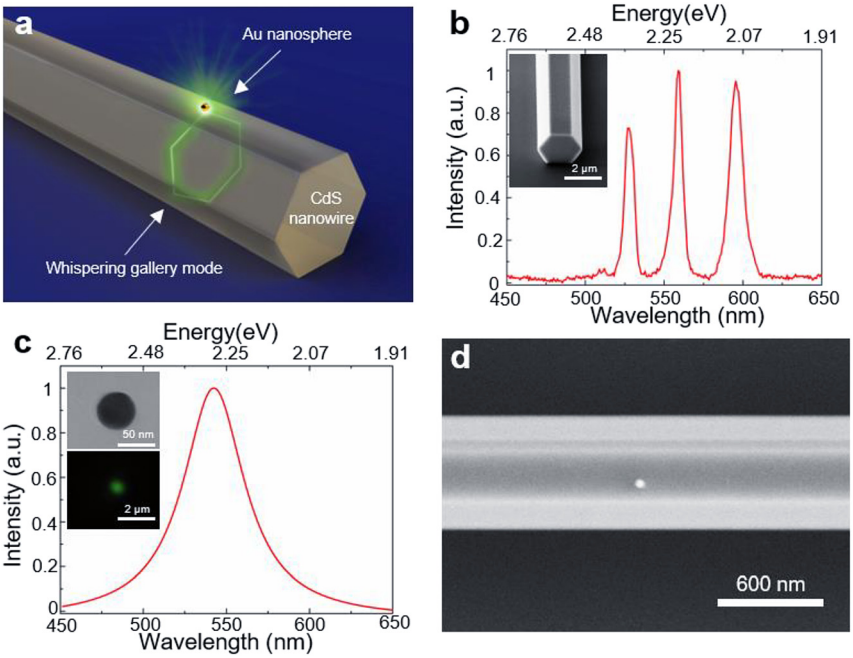

Figure 1: Hybrid strong-coupling system. (a) Schematic diagram of a coupled system consisted of an Au nanosphere and a CdS wire. (b) Dark-field scattering spectrum of a 1.5-μm-diameter CdS wire. The inset shows a scanning electron microscope (SEM) image of a CdS wire with a hexagonal cross section. (c) Typical scattering spectrum of a 50-nm-diameter Au nanosphere deposited on a glass slide presenting a line width of ~45 nm. The insets show a transmission electron microscopy (TEM) image (upper) and a dark-field optical microscope image (bottom) of a typical Au nanosphere. (d) SEM image of an as-fabricated hybrid nanosphere-nanowire structure.

spectrum of a 50-nm-diameter Au nanosphere on a glass slide. The measured LSPR peak wavelength is 542 nm, with a linewidth of 45 nm (for reference, typical scattering spectrum of a 50-nm-diameter Au nanosphere deposited on a CdS crystal is provided in Figure S4 in the Supplementary Material). By immersing a CdS wire into a dilute Au nanosphere aqueous solution for a few seconds and drying it in the open air, a hybrid structure was observed with an Au nanosphere deposited on one sidewall of a 650-nm-diameter CdS wire (Figure 1d).

3 Experimental setup and results

To investigate the spectral response of the hybrid structure, we use an unpolarized white light for side-illuminated excitation and a dark-field microscope for scattering signal collection. As shown in Figure 2a, the white light is focused onto the wire at 30° with respect to the *c*-axis of the wire. The scattered light is collected by a 100× objective and directed into a spectrometer (QE pro, Ocean Optics) and a charge-coupled device camera (DS-Filc, Nikon), respectively. Figure 2b shows a dark-field scattering image of three separated 50-nm-diameter Au nanospheres deposited on a 500-nm-diameter CdS wire, in which the scattering signal from each nanosphere can be used for studying the coupling behavior between the nanosphere and the wire. Also, since the separation between the neighboring nanospheres is much larger than the cross section of the WGM mode, there is no effective coupling between neighboring WGMs.

Hexagonal cavity of a CdS wire can support transverse magnetic (TM, electric field parallel to the c-axis) and transverse electric (TE, magnetic field parallel to the c-axis) polarized WGMs [31]. Figure 2c and d shows calculated field distribution of a TM and a TE WGMs in a 500-nm-diameter CdS wire at a resonant wavelength of 520 nm, respectively. Experimentally, the efficiency of launching WGMs in such a wire via direct free-space illumination is very low. When

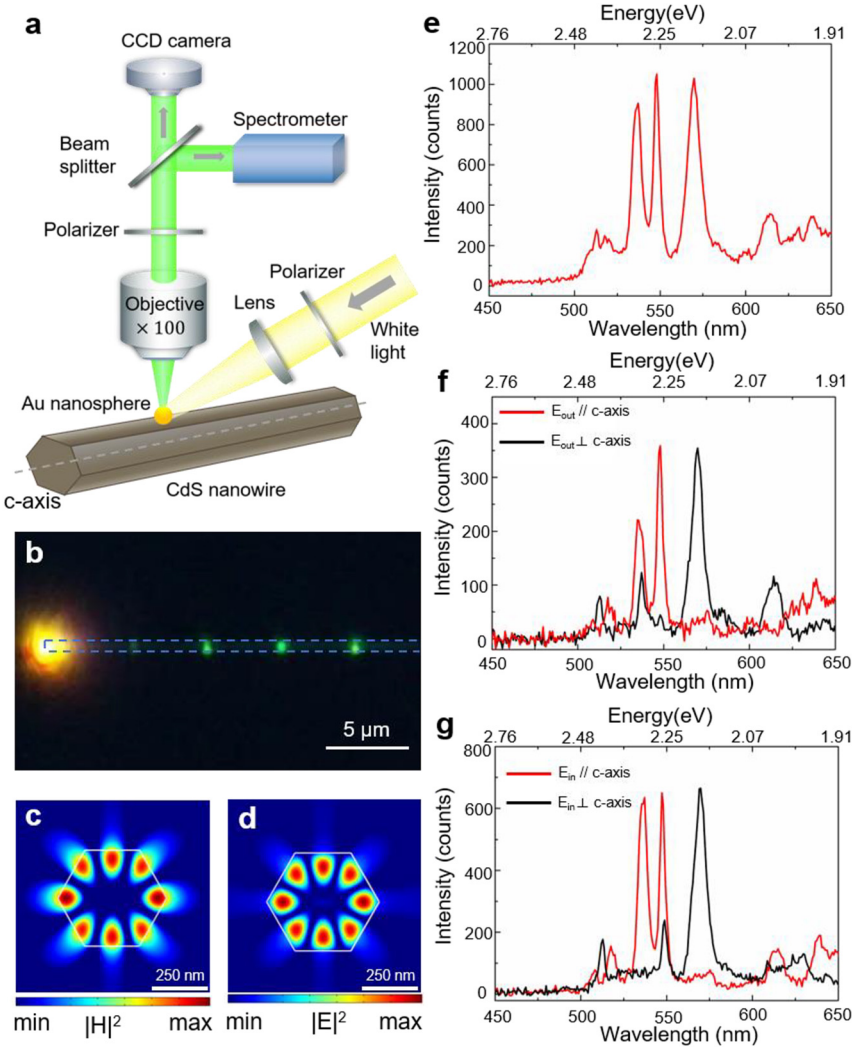

Figure 2: Optical response of the coupled system.
(a) Schematic of the side-illuminated dark-field setup for the scattering imaging and spectral analysis of the coupling system. (b) Optical microscope image of single Au nanospheres coupled to a CdS wire under excitation of white light. (c) and (d) Simulated electromagnetic field distribution of a TM (c) and a TE (d) polarized WGMs existed in a 500-nm-diameter CdS wire at a resonant wavelength of 520 nm. (e) Dark-field scattering spectrum of a 50-nm-diameter Au nanosphere coupled to a 500-nm-diameter CdS wire. (f) and (g) Dark-field scattering spectra with polarized collection (f) and excitation (g) of the above coupling system.

an Au nanosphere is deposited on the surface of the wire, it can work as an antenna to receive incident light, recirculate the light through LSPR and couple light into WGMs with a much higher efficiency. Unlike the Au nanorod used in the previous work [17], the highly symmetric Au nanosphere used here can support LSPR with three degenerate modes in free space, making it possible to couple light into both TE and TM WGMs in the wire. Figure 2e demonstrates a scattering spectrum of an Au nanosphere coupling to a 500-nm-diameter CdS wire under unpolarized excitation, in which there are three dominant resonance modes. To identify the origin of these modes, the polarization of the scattering spectrum is examined (Figure 2f). The first and second modes exhibit the same TM polarization, while the third mode shows TE polarization. The scattering spectra (Figure 2g) under polarized excitation further confirm the polarization of these modes.

The first two modes are attributed to splitting modes due to strong coupling between a TM mode of the CdS wire and an LSPR mode of the Au nanosphere (Figure 2e), and the third mode is an unsplit TE mode in a weak coupling regime. During the coupling process, partial energy of the LSPR mode radiates into the WGM of the wire cavity. The eigenmodes (E_{up} and E_{low}) of the coupling system can be estimated from a coupled oscillation model [32] (see Section 5 in the Supplementary Material). Experimentally, E_{up} (2.31 eV) and E_{low} (2.26 eV) can be obtained from the peaks of the first two modes in the scattering spectrum, and their dissipation rates (γ_1 = 17 meV and γ_2 = 36 meV) can be calculated from their corresponding linewidths of the scattering spectra fitted by Lorentzian shapes. The coupling strength can be estimated by $\Omega = E_{up} - E_{low}$ (50 meV), where the detuning of the two original modes is close to zero. In this case, $\Omega > \frac{\gamma_1+\gamma_2}{2}$ (i.e., average dissipation of the coupled system), so the interaction is in a strong coupling regime. The reason why the TE mode is not strongly coupled to the LSPR mode is that it locates much far away from the peak of the LSPR (Figure 2f and g), and it also provides a relatively weak evanescent field on the wire surface for interacting with the nanosphere (Figure 2c and d).

To investigate the coupling behavior of the hybrid system, scattering spectra of 50-nm-diameter Au nanospheres coupled individual CdS wires of different diameters are studied under TM-polarized excitation (Figure 3a–d). When the wire diameter (1.9 μm) is relatively large, the scattering spectrum of the LSPR is simply modulated by the WGMs, as a result of the coupling between the nanosphere and the wire. As the least time required for establishing the WGM estimated by the

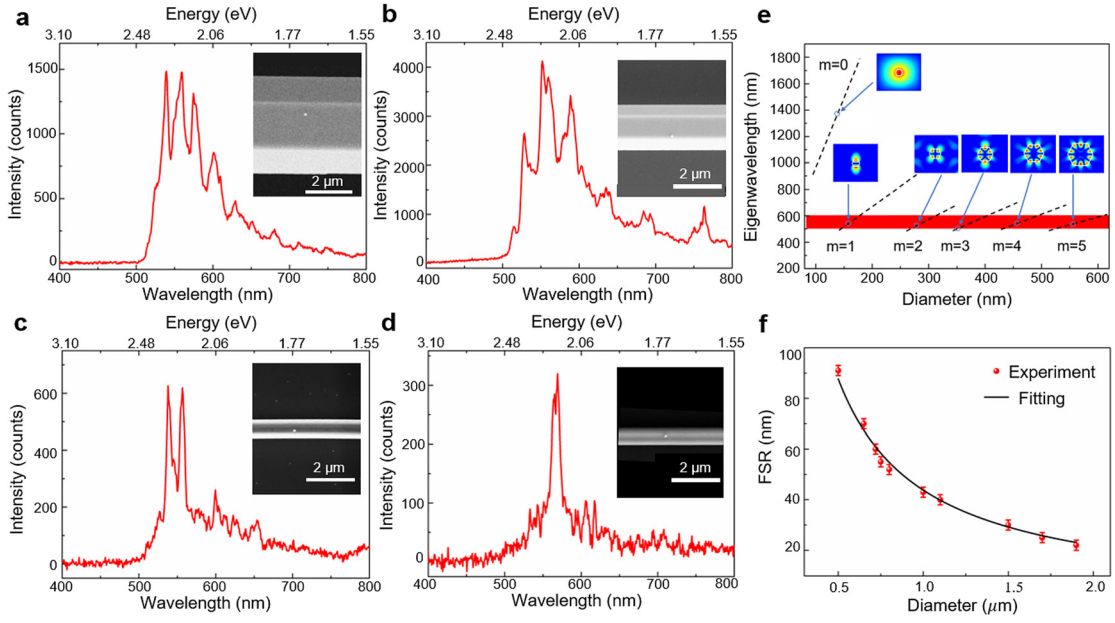

Figure 3: Coupling behavior of the hybrid system.
(a–d) Dark-field scattering spectra of single Au nanospheres coupled to CdS wires with diameters of (a) 1.9, (b) 1.1, (c) 0.6 and (d) 0.3 μm, respectively. Insets show the SEM images of the corresponding coupling system. (e) The calculated symmetric TM-polarization eigenwavelengths in CdS wire cavities with small sizes. Each eigenwavelength is labeled by an azimuthal mode number, *m*. The dash lines show the eigenwavelength of each mode number against diameters. The red shading region is the spectrum range for the LSPR of Au nanospheres. The insets are simulated field distributions for different mode numbers respectively. (f) The dependence of FSR on the diameter of CdS wires. The FSR curve fits well to a α/D function (α is ~43 nm μm).

single-cycle dwelling time of photons in a 2-μm-diameter wire (>100 fs) is much larger than the lifetime of the LSPR (~10 fs) in the Au nanosphere, the coupling behavior is difficult to be identified in the scattering spectrum. As the wire diameter decreases, the establishment time of the WGM is approaching the LSPR lifetime, and the coupling strength is also enhanced by the increasing fractional evanescent field (see Figure S5 in the Supplementary Material). When the wire diameter decreases to ~1.1 μm, evident mode splitting emerges (Figure 3b), but the splitting has not yet exceeded the average dissipation of two original modes, and the system is still in the weak coupling regime. When the wire diameter decreases further to 600 nm, strong coupling behavior is clearly seen (Figure 3c). The coupling strength (80 meV) extracted from the scattering spectrum is larger than the average dissipation ($\gamma_1 = 33$ meV, $\gamma_2 = 34$ meV). Because of the large free spectral range (FSR) of the WGM (~65 nm), only one dominant TM mode (splitted into a doublet) couples with the LSPR. When the wire diameter is reduced to 300 nm, strong coupling still exists (Figure 3d), which is the smallest WGM cavity that can strongly couple with Au nanospheres in our case. Although a thinner wire can support WGMs theoretically (see insets of Figure 3e), the cavity loss due to the diffraction becomes too large to maintain the condition for strong coupling. Figure 3f shows measured FSRs of WGMs around 550-nm wavelength with different wire diameter, fitting well to a α/D function (α is a fitting constant and D is the wire diameter). The experimentally fitted α is (~43 nm μm), in good agreement with the theoretical calculation ($\alpha = \frac{2\lambda^2}{3\sqrt{3}\, n_{\text{eff}}}$ ~ 45 nm μm, λ ~ 550 nm, and n_{eff} ~ 2.6).

To map the dispersion of the coupled system, we measured its temperature-dependent dark-field scattering spectra in a cryostat system (ST-500, Janis). For the WGMs in a CdS nanowire, as temperature increases, the peaks of resonance modes redshift because of the positive temperature-dependent coefficient of the refractive index (~4×10^{-4} K^{-1}) of CdS [33], which can change the detuning between the WGMs and the LSPR mode, while the thermal expansion effect on the CdS-nanowire-cavity size (coefficient of thermal expansion [34], ~4.6×10^{-5} K^{-1}) can be ignored. Figure 4a shows the calculated dispersion of TM modes in a 550-nm-diameter CdS nanowire, in which a

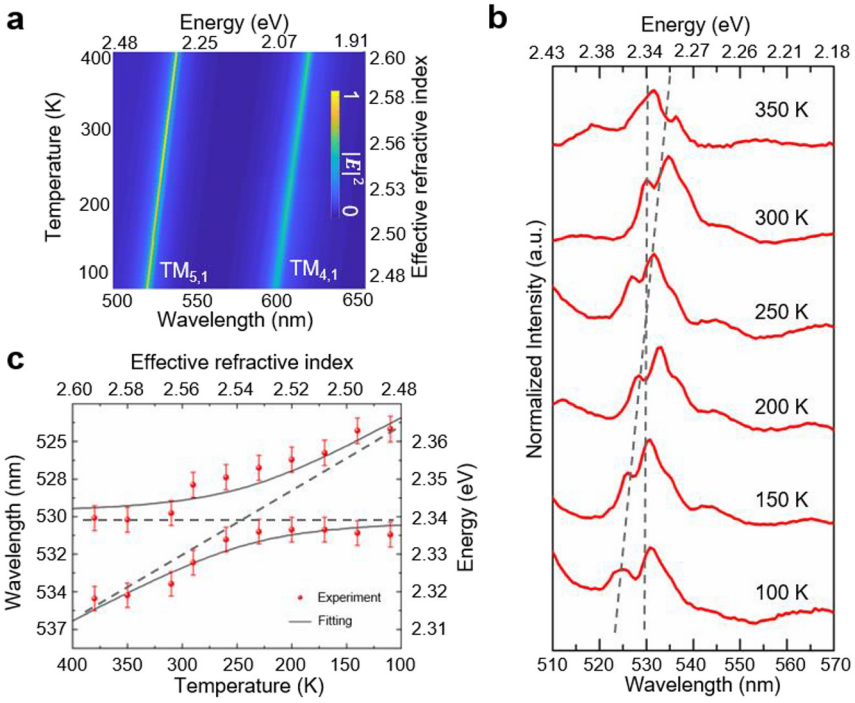

Figure 4: Temperature-dependent dispersion behavior of the coupled system.
(a) Calculated dispersion curve of WGMs in a 550-nm-diameter CdS wire with temperature increasing from 100 to 400 K. (b) Temperature-dependent dark-field scattering spectra of an Au nanosphere coupled to a 550-nm-diameter CdS wire. The temperature is scanned from 100 to 350 K with a step of 50 K. The gray dash lines denote the peak wavelengths of the uncoupled LSPR mode (vertical line) and the $TM_{5,1}$ WGM (oblique line), respectively. (c) Calculated dispersion of the $TM_{5,1}$ WGM coupling with the LSPR mode using the coupled oscillation model to fit the experimental data. The experimental data (red dots) is extracted from (b). The dash lines denote the peak wavelengths of uncoupled LSPR mode (horizontal line) and the $TM_{5,1}$ WGM (oblique line), respectively. The experimental error comes from the determination of spectrum peaks.

$TM_{5,1}$ and a $TM_{4,1}$ modes ($TM_{m,r}$: m is the azimuthal mode number and r is the radial number) redshift ~15 nm from 100 to 400 K. For comparison, the LSPR peak of a 50-nm-diameter Au nanosphere is almost temperature independent [35] (see Figure S6 in the Supplementary Material).

Figure 4b shows the temperature-dependent scattering spectra of an Au nanosphere coupled with a 550-nm-diameter nanowire. Initially, the two modes in Figure 4b follow the dispersion behavior of the uncoupled WGM and LSPR modes respectively at relatively high temperatures (about over 320 K) due to a large detuning. As the temperature decreases, the modes deviate from the original dispersions and enter the strong coupling region, with an evident anticrossing behavior in the dispersion curve (Figure 4c), agreeing well with the coupled oscillation model. The coupling strength (28 meV) is larger than the average dissipation (γ_1 = 17 meV, γ_2 = 30 meV), confirming the occurance of the strong coupling in the coupled system.

4 Conclusion

In conclusion, we have demonstrated strong coupling of an Au nanosphere to a CdS nanowire with a mode splitting up to 80 meV at room temperature. The coupling of a 50-nm-diameter Au nanosphere to single CdS wires with different diameters (0.3–1.9 μm) were investigated. Strong coupling between WGM and LSPR modes is observed with wire diameter between 300 and 600 nm, offering a scheme to realize a strongly coupled hybrid "photon–plasmon" system with ultracompactness. The coupling scheme can be applied to many other semiconductor nanowires, and the LSPR modes in a nanosphere can be selectively coupled with TE and TM WGMs in the nanowire. Owing to the high optical gain and nonlinearity in semiconductor nanowires, this kind of strong-coupling hybrid structures may open new opportunities for a variety of applications such as ultracompact low-threshold nanolasers and nonlinear optical devices.

Author contributions: All authors have given approval to submission of the manuscript.

Research funding: This research was supported by the National Natural Science Foundation of China (No. 61635009), the National Key Research and Development Project of China (No. 2018YFB2200400), Natural Science Foundation of Zhejiang Province (No. LR21F050002), and the Fundamental Research Funds for the Central Universities.

Conflict of interest statement: The authors declare no conflicts of interest.

References

[1] G. A. Wurtz, P. R. Evans, W. Hendren, et al., "Molecular plasmonics with tunable exciton-plasmon coupling strength in J-aggregate hybridized Au nanorod assemblies," *Nano Lett.*, vol. 7, pp. 1297–1303, 2007.

[2] A. Delga, J. Feist, J. Bravo-Abad, and F. J. Garcia-Vidal, "Quantum emitters near a metal nanoparticle: strong coupling and quenching," *Phys. Rev. Lett.*, vol. 112, 2014, Art no. 253601.

[3] X. F. Fan, W. T. Zheng, and D. J. Singh, "Light scattering and surface plasmons on small spherical particles," *Light Sci. Appl.*, vol. 3, p. e179, 2014.

[4] G. Zengin, M. Wersäll, S. Nilsson, T. J. Antosiewicz, M. Käll, and T. Shegai, "Realizing strong light-matter interactions between single-nanoparticle plasmons and molecular excitons at ambient conditions," *Phys. Rev. Lett.*, vol. 114, p. 157401, 2015.

[5] D. Zheng, S. P. Zhang, Q. Deng, M. Kang, P. Nordlander, and H. X. Xu, "Manipulating coherent plasmon-exciton interaction in a single silver nanorod on monolayer WSe_2," *Nano Lett.*, vol. 17, pp. 3809–3814, 2017.

[6] R. M. Liu, Z. K. Zhou, Y. C. Yu, et al., "Strong light-matter interactions in single open plasmonic nanocavities at the quantum optics limit," *Phys. Rev. Lett.*, vol. 118, 2017, Art no. 237401.

[7] C. E. Talley, J. B. Jackson, C. Oubre, et al., "Surface-enhanced Raman scattering from individual Au nanoparticles and nanoparticle dimer substrates," *Nano Lett.*, vol. 5, pp. 1569–1574, 2005.

[8] J. F. Li, Y. F. Huang, Y. Ding, et al., "Shell-isolated nanoparticle-enhanced Raman spectroscopy," *Nature*, vol. 464, pp. 392–395, 2010.

[9] B. Sepúlveda, P. C. Angelomé, L. M. Lechuga, and L. M. Liz-Marzán, "LSPR-based nanobiosensors," *Nano Today*, vol. 4, pp. 244–251, 2009.

[10] G. Kewes, K. Herrmann, R. Rodríguez-Oliveros, A. Kuhlicke, O. Benson, and K. Busch, "Limitations of particle-based spasers," *Phys. Rev. Lett.*, vol. 118, 2017, Art no. 237402.

[11] H. Wu, Y. X. Gao, P. Z. Xu, et al., "Plasmonic nanolasers: pursuing Extreme lasing conditions on nanoscale," *Adv. Opt. Mater.*, vol. 7, 2019, Art no. 1970064.

[12] Y. X. Gao, H. Wu, N. Zhou, et al., "Single-nanorod plasmon nanolaser: a route toward a three-dimensional ultraconfined lasing mode," *Phys. Rev. A*, vol. 102, 2020, Art no. 063520.

[13] H. Baida, D. Mongin, D. Christofilos, et al., "Ultrafast nonlinear optical response of a single gold nanorod near its surface plasmon resonance," *Phys. Rev. Lett.*, vol. 107, 2011, Art no. 057402.

[14] Y. F. Xiao, C. L. Zou, B. B. Li, et al., "High-Q exterior whispering-gallery modes in a metal-coated microresonator," *Phys. Rev. Lett.*, vol. 105, 2010, Art no. 153902.

[15] F. H. Alast, M. Nikkhah, X. Li, et al., "Hybrid loss-compensated plasmonic device," *Adv. Opt. Mater.*, vol. 7, 2018, Art no. 1801189.

[16] P. Peng, Y. C. Liu, D. Xu, et al., "Enhancing coherent light-matter interactions through microcavity-engineered plasmonic resonances," *Phys. Rev. Lett.*, vol. 119, 2017, Art no. 233901.

[17] P. Wang, Y. P. Wang, Z. Y. Yang, et al., "Single-band 2-nm-Line-Width plasmon resonance in a strongly coupled Au nanorod," *Nano Lett.*, vol. 15, 2015, Art no. 7581–7586.

[18] J. H. Yang, Q. Sun, K. Ueno, et al., "Manipulation of the dephasing time by strong coupling between localized and propagating surface plasmon modes," *Nat. Commun.*, vol. 9, p. 4858, 2018.
[19] S. Kéna-Cohen, S. A. Maier, and D. D. C. Bradley, "Ultrastrongly coupled exciton-polaritons in metal-clad organic semiconductor microcavities," *Adv. Opt. Mater.*, vol. 1, pp. 827–833, 2013.
[20] K. J. Vahala, "Optical microcavities," *Nature*, vol. 424, pp. 839–846, 2003.
[21] S. C. Yang, Y. Wang, and H. D. Sun, "Advances and prospects for whispering gallery mode microcavities," *Adv. Opt. Mater.*, vol. 3, pp. 1136–1162, 2015.
[22] J. F. Lu, C. X. Xu, J. Dai, et al.,"Plasmon-enhanced whispering gallery mode lasing from hexagonal Al/ZnO microcavity," *ACS Photonics*, vol. 2, pp. 73–77, 2015.
[23] A. B. Vasista and W. L. Barnes, "Molecular monolayer strong coupling in dielectric soft microcavities," *Nano Lett.*, vol. 20, pp. 1766–1773, 2020.
[24] K. Srinivasan and O. Painter, "Linear and nonlinear optical spectroscopy of a strongly coupled microdisk-quantum dot system," *Nature*, vol. 450, pp. 862–865, 2007.
[25] T. Aoki, B. Dayan, E. Wilcut, et al., "Observation of strong coupling between one atom and a monolithic microresonator," *Nature*, vol. 443, pp. 671–674, 2006.
[26] C. Junge, D. O'Shea, J. Volz, and A. Rauschenbeutel, "Strong coupling between single atoms and nontransversal photons," *Phys. Rev. Lett.*, vol. 110, 2013, Art no. 213604.
[27] W. G. Farr, M. Goryachev, D. L. Creedon, and M. E. Tobar, "Strong coupling between whispering gallery modes and chromium ions in ruby," *Phys. Rev. B*, vol. 90, 2014, Art no. 054409.
[28] Y. N. Xia, P. D. Yang, Y. G. Sun, et al., "One-Dimensional nanostructures: synthesis, characterization, and applications," *Adv. Mater.*, vol. 15, pp. 353–389, 2003.
[29] M. Willander, O. Nur, Q. X. Zhao, et al., "Zinc oxide nanorod based photonic devices: recent progress in growth, light emitting diodes and lasers," *Nanotechnology*, vol. 20, 2009, Art no. 332001.
[30] T. Nobis, E. M. Kaidashev, A. Rahm, M. Lorenz, and M. Grundmann, "Whispering gallery modes in nanosized dielectric resonators with hexagonal cross section," *Phys. Rev. Lett.*, vol. 93, 2004, Art no. 103903.
[31] C. Czekalla, T. Nobis, A. Rahm, et al.,"Whispering gallery modes in zinc oxide micro- and nanowires," Phys. Status Solidi B, vol. 247, pp. 1282–1293, 2010.
[32] D. M. Coles, N. Somaschi, P. Michetti, et al., "Polariton-mediated energy transfer between organic dyes in a strongly coupled optical microcavity," Nat. Mater., vol. 13, pp. 712–719, 2014.
[33] D. W. Langer, "Temperature and pressure dependence of the index of refraction of CdS," J. Appl. Phys., vol. 37, pp. 3530–3532, 1966.
[34] P. V. B. Lakshmi and K. Ramachandran, "On the thermal expansion of CdS by experiment and simulation," Cryst. Res. Technol., vol. 41, pp. 498–504, 2006.
[35] J. X. Wen, H. Wang, W. L. Wang, et al., "Room-temperature strong light-matter interaction with active control in single plasmonic nanorod coupled with two-dimensional atomic crystals," Nano Lett., vol. 17, pp. 4689–4697, 2017.

Supplementary Material: The online version of this article offers supplementary material (https://doi.org/10.1515/nanoph-2021-0214).